DELPHI Collaboration DELPHI 96-158 PHYS 651
18 November, 1996

Colour Reconnection in String Model

Šárka Todorova-Nová

Nuclear Centre of Charles University, Prague
CRN Strasbourg [1]

Abstract

Physical manifestations of colour reconnection at LEP200 are analysed as a function of the basic parameters of a reconnection model based on strings. Reconnection effects in hadronic decays of Z^0/γ at LEP1 are discussed. An attempt is made to extract the reconnection probability (free parameter of the model) from experimentally measured 'colour reconnected' heavy meson decays.

[1] e-mail: nova@crnvax.in2p3.fr

Contents

1 Introduction

Colour reconnection is the term used for strong interaction between independent colour singlets, usually before hadron formation. In hadronic decays of high energy particles colour reconnection can recombine partons from different parton showers . After fragmentation, the resulting hadrons carry therefore a mixture of energy-momentum of both original showers. Such an effect clearly complicates the experimental measurement of the properties of the primary partons.

At LEP200, colour reconnection is a potential dangerous source of systematic error in the analysis of hadronically decaying WW pairs. Simultaneously, however, the effect represents also an interesting QCD problem.

The possibility of calculating the effect in the frame of QCD is rather limited : the comparison of the absolute value of the interference and of the non-interference terms for the 2 gluon exchange showed [1] that reconnection is strongly suppressed at the early stage of the development of the parton shower ($\sigma_{rec}/\sigma_{no-rec} \ll 10^{-3}$). However, the interference (interpreted as colour reconnection) can become more important in higher orders and especially at the non-perturbative level. The obvious approach is to use existing phenomenological models of hadronization and to try to implement colour reconnection in a "reasonable" way. This is done either by looking at the space-time development of the shower and by imposing reconnection as a function of the distance between coloured objects (as in JETSET, HERWIG), or by reducing the length of strings in momentum space (as in ARIADNE).

The task is of course complicated by the lack of experimental input. So far, the only experimental evidence of colour reconnection is the measurement of heavy meson 'reconnected' decays (such as $B \to J/\Psi X$). The size of the effect in high energy processes has yet to be estimated and it is the aim of this paper to help to set some boundaries on it.

The work is based on a previous study [1], where the fundamental features of the string-based model of colour reconnection were formulated. The following section contains a brief review of this model, extended to multiple reconnection and with inclusion of the space-time development of the shower.

2 Simulation of colour reconnection

The details of the string model will not be discussed here. It is sufficient to point out that the description of the colour potential with help of strings stretched via partons is at the heart of the successful and widely used phenomenological model of hadronization [2].

In short, from the very beginning of the development of a parton shower, we consider partons to be connected by a string according to colour flow. The string is considered to be a set of

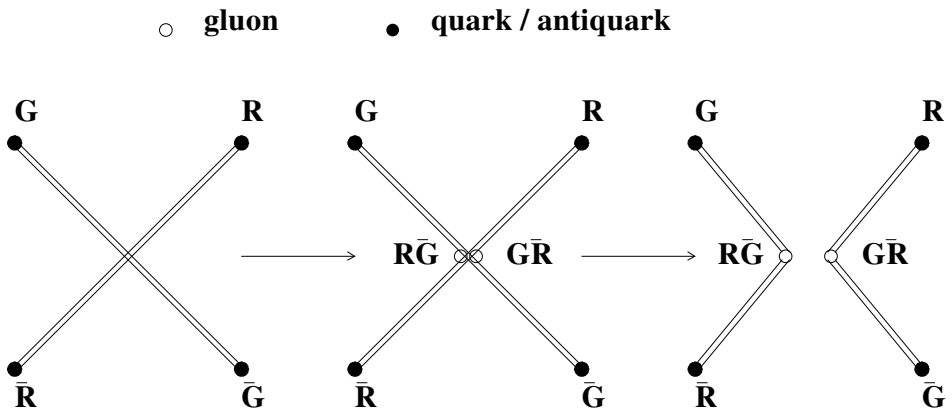

Figure 1: *Colour reconnection as an exchange of two gluons.*

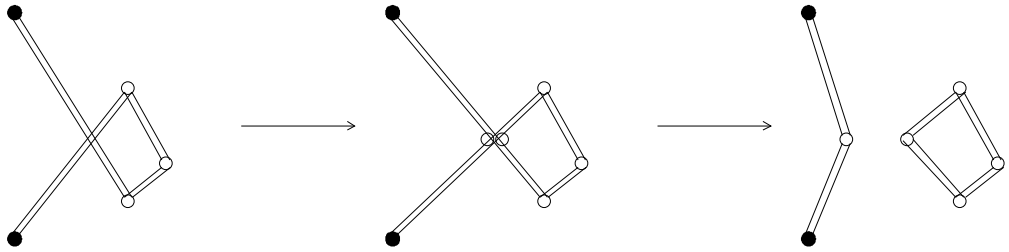

Figure 2: *Self-interaction leading to the string - production of glueball.*

straight string pieces defined by the position of the end-point partons. Reconnection of strings means that two original strings (more precisely two string pieces , i.e. parts of a string connecting neighbouring partons in each string) break and reconnect to form new, rearranged strings.

Two extreme types of strings (scenario I, II in [1]), corresponding to two different types of

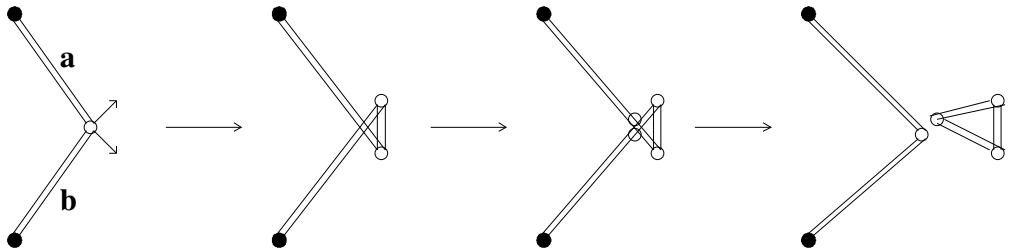

Figure 3: *Production of a glueball after gluon branching.*

QCD vacuum (analogous to superconductors of type I and II), are studied . The **reconnection probability** is supposed to be related to the distance between strings (the dependence on the colour structure will be discussed later):

- **"Flux tubes"**(type I): strings are viewed as cylindrical bags with a transverse dimension of hadronic size and a gaussian fall of the colour field density in the transverse direction (as an approximation the colour field is assumed to be uniform along the string). The string is thus characterised by a field Ω whose expression is:

$$\Omega(\vec{x},t) = \exp\left(\frac{-r^2}{2.r_{had}^2}\right).\exp\left(\frac{-t^2}{\tau_{frag}^2}\right) \tag{1}$$

  where $r_{had} \simeq 0.5$ fm ...transverse dimension of a string (e.g. from lattice QCD calculations)
  $\tau_{frag} \simeq 1.5$ fm ..mean life time of a string (given by fragmentation parameters).

  The probability of reconnection between strings (string pieces) of the type 'flux tube' is related to the overlapping of their colour fields

$$p = 1 - \exp(-R_s.I) \tag{2}$$

  where

$$I = \int d\Omega_1(\vec{x},t)d\Omega_2(\vec{x},t)d\vec{x}dt \tag{3}$$

  and the reconnection strength R_s is a free parameter of the model.

  The results presented in this note are based on an extension of the model used in [1]. The latter was improved by allowing the overlapping of strings to be numerically integrated event by event and separately for each pair of string pieces.

- **"Vortex lines"**(type II): strings with thin cores in which all topological information is stored, surrounded by a chromoelectric field with exponential fall in the transverse direction. Compared to the model used in [1], the present calculation allowed the diameter of the core to be finite.

  Strings of the type 'vortex line' are reconnected always when their cores intersect. The minimal distance between string pieces is found analytically and compared to the given diameter of the core.

The most important extension introduced in the model is the implementation of the space-time evolution of the parton showers based on the formulae for the mean life time of partons in the shower:

$$t_{life} = \frac{\hbar E}{q^2} \tag{4}$$

where q^2 is the virtuality and E the energy of the parton.

Starting from the decay of the original particle (W boson), the probability of reconnection is evaluated for each pair of string pieces using steps given by the time intervals between two following branchings in the shower. If the probability appears to be sufficiently high for a given pair, the string pieces are reconnected, the colour flow is rearranged and the whole procedure continues until the last parton is emitted (or the whole string fragmentated). The quark masses are neglected as well as the string-parton interaction ('yo-yo' effect).

Multiple reconnection has been added to the original model (including back-reconnection) and the whole process is limited by the life time τ of the string which is generated according to the expression:

$$\mathcal{P}_{fragm}(\tau)d\tau = \frac{2}{\tau^2_{frag}} \ \exp(-\frac{\tau^2}{\tau^2_{frag}}) \ \tau d\tau \tag{5}$$

This is an approximation, since the fragmentation is not an instantaneous process.

The problem of colour structure (final strings/glueballs have to be colour singlets) is – at least partly – solved by assuming that the reconnection mechanism is an exchange of two gluons born out of vacuum (Fig. 1). These gluons are not explicitly included in the simulation for the moment but can be given the appropriate energy/momentum during further steps of the model building.

The possibility of self-interaction of a string has been implemented. The product of such an interaction, a 'prefragmented' glueball (see Fig. 2), can take part in another reconnection according to the same rules as for 'usual' strings.

The self-interaction of a string opens a new area for studies: such an internal shower reconnection can be interpreted as a kind of higher order correction in hadronic decays of a single particle, such as the Z^0.

3 Colour reconnection in WW hadronic decays

The measurement of the W mass via direct reconstruction in the case where both W's decay hadronically could in principle be disturbed by the uncertainty related to colour reconnection. The precision aimed on the W mass at LEP2 is around 50 MeV in the purely hadronic final state (statistics and systematics combined [3]). To achieve this precision, the uncertainty due to colour reconnection (which was supposed to be as high as $\pm$ 100 MeV [3]), as well as to the Bose-Einstein effect (which is not properly simulated either) has to be pushed down substantially.

In this section, a study of the consequences of colour reconnection for the W mass measurement performed at the generator level is presented.

W^+W^- pairs and their decay products were generated with the PYTHIA version 5.6. The

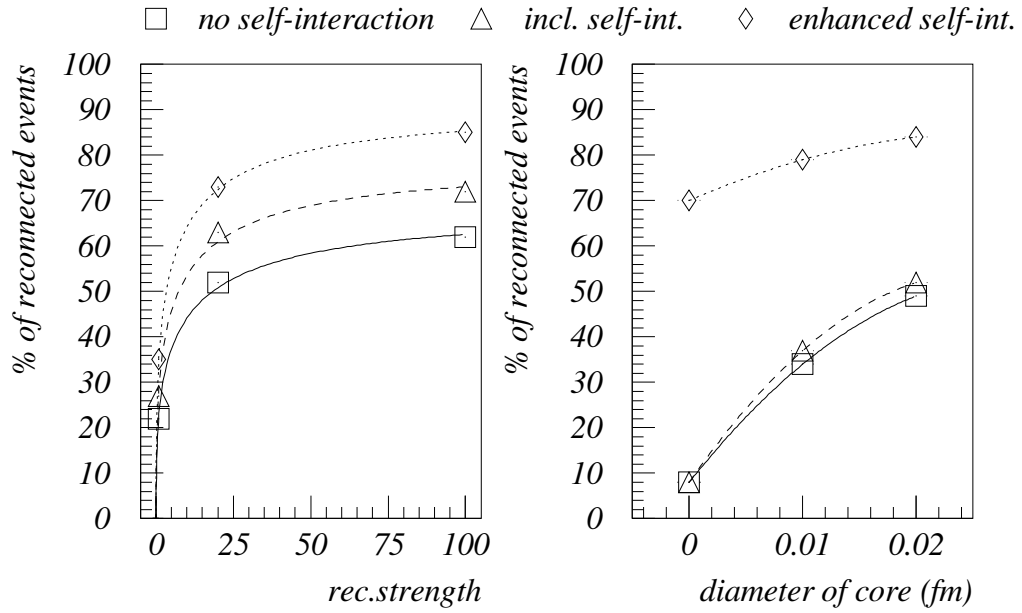

Figure 4: *Relative number of reconnected hadronic WW events as a function of the reconnection strength R_s (flux tubes) and of the diameter of the core (vortex lines). Three scenarios are considered: 1) no self-interaction, 2) with self-interaction of strings, 3) same as 2) but with reconnection after gluon branching (Fig.3).*

colour reconnection procedure was implemented between the parton showering and the fragmentation (JETSET 7.4 with the DELPHI tuning was used [4]). The original goal of this study was to estimate the 'pure' effect of colour reconnection. So, only 'clean' 4 jet events were used in the analysis. The events were selected by requesting a minimal jet energy of 20 GeV and a minimal angular separation between jets of 0.5 rad. In addition, ISR radiation was switched off. The combinatorial background was suppressed with the use of the generator information on the quark momentum: the product of invariant masses of the quark-jet system was minimized for this purpose. Comparative studies were performed by first generating a parton shower configuration without colour reconnection and, second, by repeating the configuration with colour reconnection activated (in order to reduce statistical fluctuations).

Since there are quite a lot of parameters inside the model, only the most significant ones were studied in detail: these are the reconnection strength for flux tubes and the transverse dimension of the strings in case of vortex lines. Other parameters were kept at constant value (such as the transverse dimension of strings - 0.5 fm - in the flux tube model) or derived from tuned parameters of JETSET (e.g. parton shower cut-off = 1.56 GeV, mean fragmentation time

of strings = 1.5 fm/c).

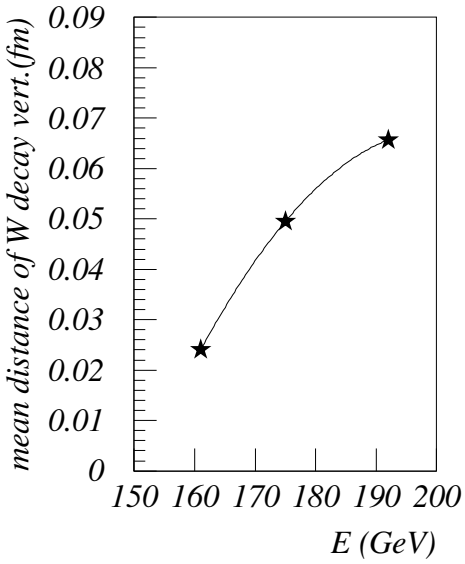

Figure 5: *Mean distance of W^+W^- decay vertices as a function of the c.m. energy.*

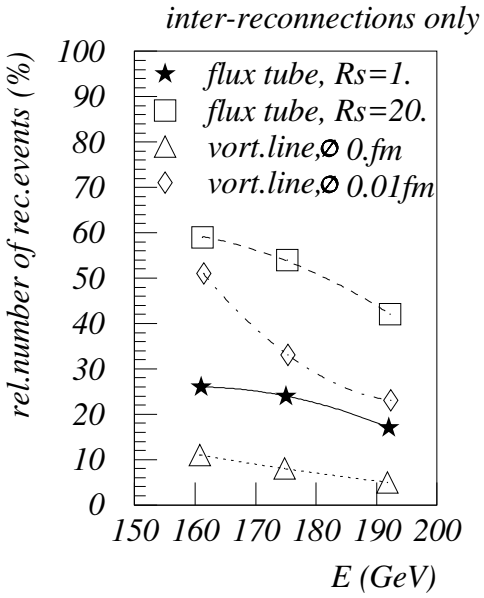

Figure 6: *Relative number of reconnected events as a function of the c.m. energy (without self-interaction).*

3.1 Reconnection probability

The fraction of events where at least one reconnection occurs between W's ('inter-reconnection') is plotted in Fig. 4 for a c.m.energy of 175 GeV (full line). In the case of flux tubes, the distribution rises quickly with the reconnection strength (R_s) and reaches a plateau (corresponding to roughly 60 % of events reconnected).

Vortex lines reconnect more and more as their transverse dimension increases. However, if they are as thick as to overlap immediately after the W decay the simulation becomes unreliable.

If the reconnection inside one shower is allowed ('self-interaction'), the fraction of events with reconnection is enhanced (dashed lines in Fig. 4). There is one special case of reconnection inside a shower : the production of a glueball just after gluon splitting (Fig. 3). While this does not really influence the proportion of events reconnected in scenario I (flux tubes), a huge increase of the reconnection rate is observed for vortex lines . This is because, at the moment of the gluon splitting, string pieces a, b (Fig. 3) are close enough to get always reconnected. It would

of course be possible to solve technically this difficulty had we had a more precise idea about the correct reconnection rate . At present, either such specific reconnections are allowed and the corresponding distributions should be regarded as an extreme limit due to glueball production, or they are forbidden (concerns vortex lines only !).

With increasing c.m. energy, the amount of events with a WW inter-reconnection decreases as expected (showers are better separated at higher energies), as can be seen in Fig. 5 and 6.

3.2 Systematic shift in the reconstructed W mass

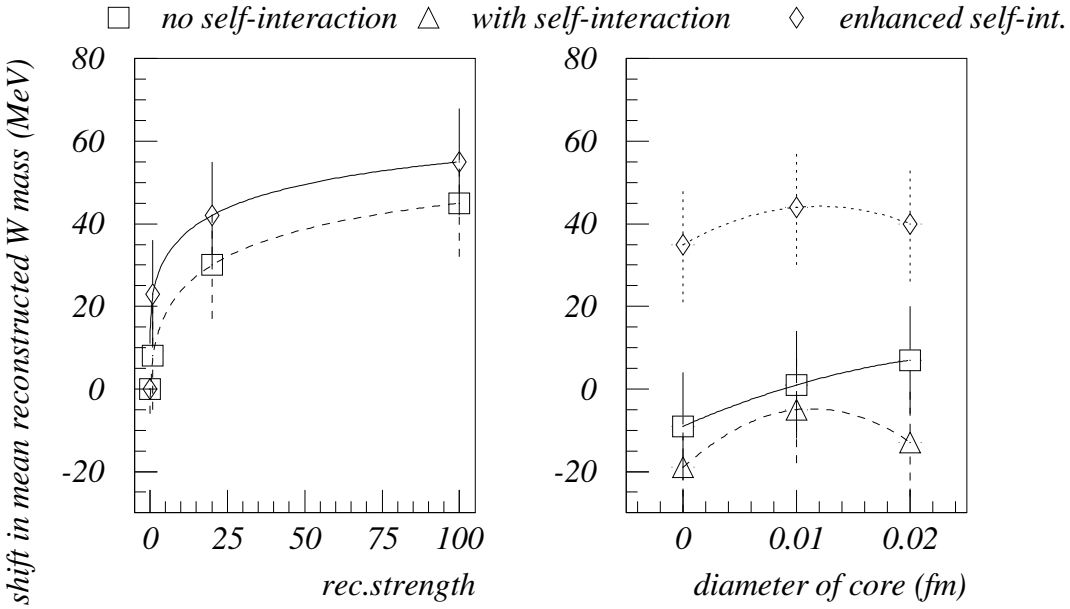

Figure 7: *Systematic shift in the mean reconstructed W mass as a function of the reconnection strength (flux tubes).*

Figure 8: *Systematic shift in the mean reconstructed W mass as a function of the diameter of the core (vortex line).*

Samples of 100.000 generated events were used to estimate the systematic shift in the reconstructed W mass (about 60% of the sample satisfying the selection criteria). Distributions of the mean W mass, defined as

$$\bar{m}_W = 0.5(m_{W^+} + m_{W^-}) \tag{6}$$

obtained with and without reconnection were fitted with a Breit-Wigner function multiplied

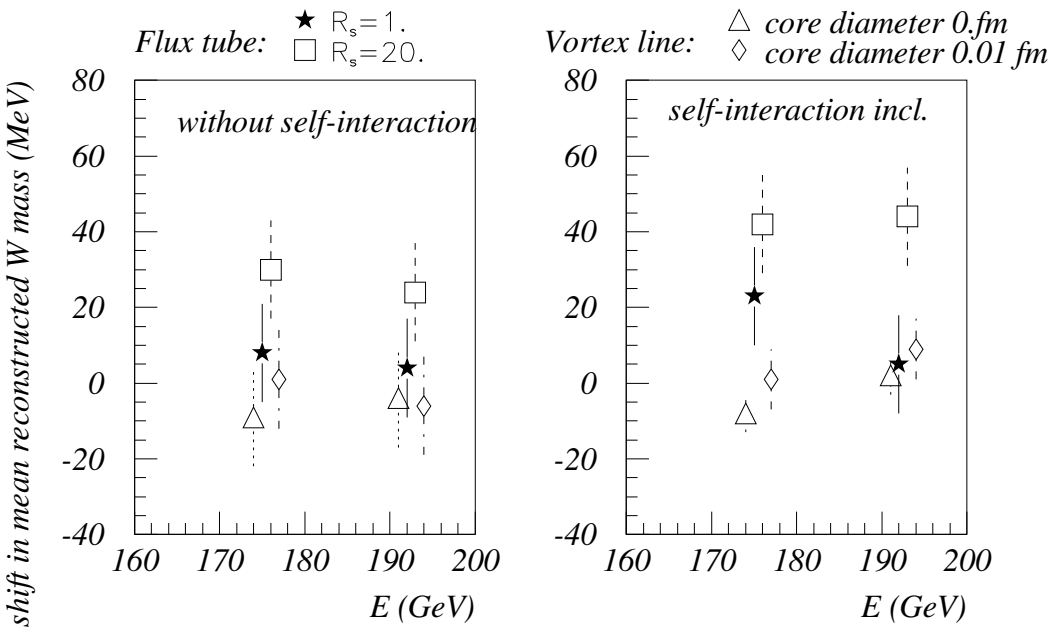

Figure 9: *Systematic shift in the mean reconstructed W mass as a function of the c.m. energy: a) without self-interaction of strings, b) with self-interaction of strings .*

by a phase space factor:

$$f(m) = N \cdot \frac{m^2 \frac{\Gamma}{M_W}}{(m^2 \frac{\Gamma}{M_W})^2 + (m^2 - M_W^2)^2} \cdot \sqrt{1 - 4(\frac{m}{E_{cm}})^2} \tag{7}$$

The fitted values of the W mass (m) were compared with each other.

Fig. 7, 8 show the systematic shift in the mean W mass for the two reconnection scenarios as a function of their major free parameters. Here again, a kind of plateau appears for flux tubes as the reconnection strength increases, allowing to set -in principle- an upper limit. The plateau height is influenced by the parton shower cut-off and by the mean fragmentation time of strings, which define the parton multiplicity and the time-space interval available for reconnection. There is probably no easy way out from this dependence of the results. At present, there is no other approach than to rely on a tuning of the generator parameters on distributions of real data.

In case of vortex lines (Fig. 8) without self-interaction the shift is negative with a slight tendency to increase with the diameter of the core (the available statistics doesn't allow to conclude). If self-interaction of the string is enhanced (by glueball production), the systematic shift becomes positive and of the order of the saturation value predicted for flux tubes. This is a bit surprising since self-interaction should not in principle change the total energy/momentum

of the W boson. The observed shift arises from different event topology (for example, the fraction of 'lost' particles, i.e. particles wrongly assigned during reconstruction varies with colour reconnection).

While this example is an extreme case, the interplay between reconnection and reconstruction generally seems to limitate the possibility of a universal estimation of the systematic error on the W mass. A detector simulation is needed; a recent study performed in OPAL [5] shows that the shift measured experimentally can be much larger than the shift estimated at the generator level, due to the constraint fit performed on the data or due to the effect in 5- and more- jet events. The exact reasons are still to be investigated.

In addition, there is an uncertainty in the fit of the W mass distribution: the shape of the distribution is distorted by many effects (including colour reconnection) and it is not easy to fit it with a simple function (i.e. with a small number of parameters). On the other hand, fitting with a complicated function may lead to unstable results.

Therefore, the results presented here need to be studied again once the reconstruction method has been applied.

The energy dependence of the systematic shift in the mean W mass is shown in Fig. 9. With the statistics used for the study (100-200 thousands of W pairs) no clear energy dependence can be seen.

3.3 The Λ measure and the charged multiplicity

The multiplicity of final particles in the string fragmentation model is related to the string invariant mass, more conveniently expressed by the Λ measure

$$\Lambda = \sum_{string-pieces} ln(1 + m_i^2/m_0^2) \tag{8}$$

where m_i is the invariant mass of the string piece and m_0 is a constant .

The charged multiplicity (and Λ as well) decreases as the amount of reconnection increases, as can be seen on Fig. 10, 11.

The fact that reconnection tends to decrease Λ is rather interesting since no explicit request for a lower invariant mass of the reconnected string was made. On the other hand, reconnection models working in momentum space (ARIADNE) usually require a decrease in Λ as a condition for reconnection.

The final charged multiplicity can drop by as much as 8 % when the reconnection rate is high. At least half of the effect is due to the self-interaction of strings.

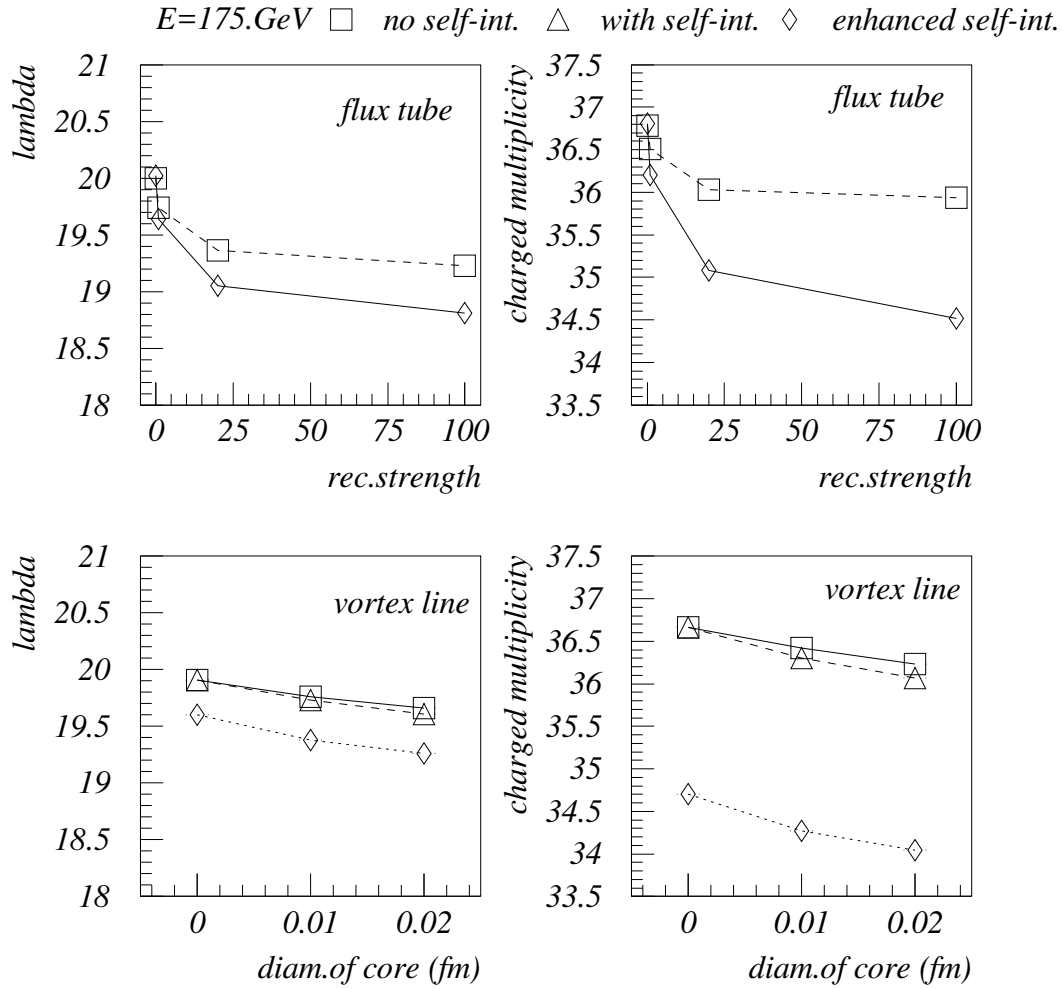

Figure 10: *Decrease of* Λ *and of the charged multiplicity as a function of the reconnection strength* R_s *(flux tubes) and of the core diameter (vortex lines).*

3.4 Discussion of results

The original study [1] of the effect of colour reconnection on the W mass determination concluded that the expected uncertainty on the W mass measurement is about 40 MeV. This number was obtained when also accounting for the uncertainty at the perturbative level of the process (estimated to 5 MeV from a theoretical calculation), for the uncertainty coming from the interplay between the perturbative and the non-perturbative parts (guessed to be 5 MeV) and, finally, for the shift observed in the simulation for a 'reasonable' reconnection rate (found to be 30 MeV).

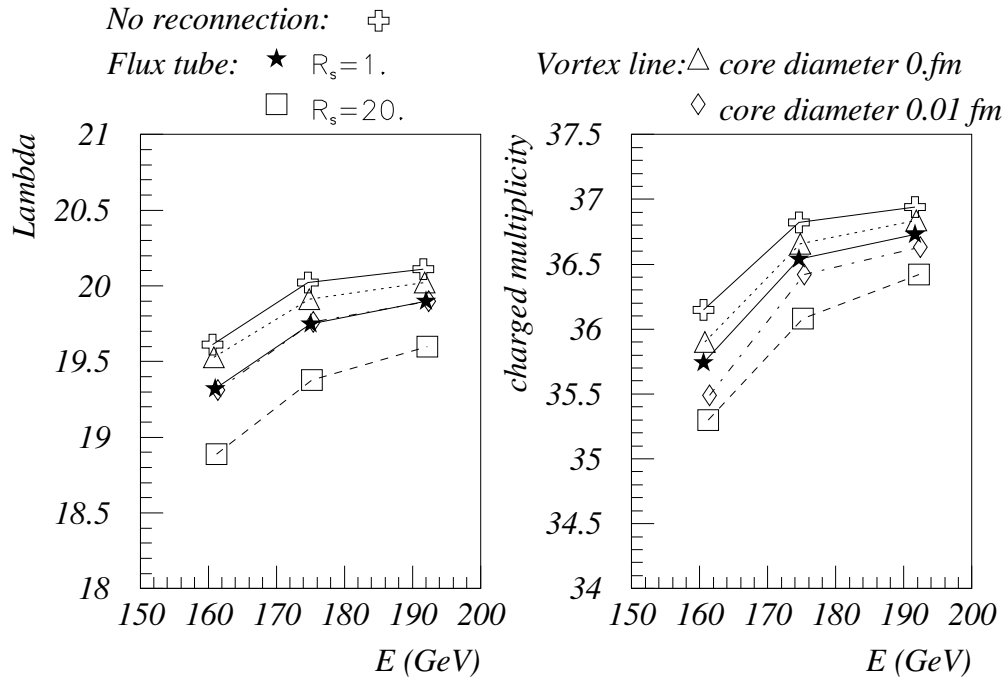

Figure 11: Λ *as function of the c.m.energy in various colour reconnection schemes.*

Figure 12: *Charged multiplicity as function of the c.m.energy in various colour reconnection schemes.*

There are several apparent weak points in this conclusion: for instance, in [1] the 'reasonable' reconnection rate in the flux tube scenario is given by the reconnection rate observed in the vortex line scenario, which happens to correspond to a reconnection strength $R_s = 0.6$. Actually there is no apparent reason why it should be so. Also, in the scenario with flux tubes, the integration of overlaps of colour fields was not done on an event by event basis but averaged over the event sample generated. The space-time evolution of the shower was not taken into account. Moreover, the uncertainty on the W mass was taken as the mean value of the distribution of the difference between the generated and the reconstructed mean W mass of each event. This method does not take into account the shape of the W mass distribution and, as it comes out from a closer study, tends to underestimate [3] the uncertainty on the W mass.

The improvement of the simulation had the following effects:

- the integration of the overlaps event by event slowed down considerably the calculation speed of the procedure but permitted a detailed study of multiple reconnection and of the individual topology of the events. The uncertainty on the W mass remained roughly the same.

- the implementation of multiple reconnection decreased the effect of reconnection by half ; such a decrease can be explained intuitively by re-reconnection (which may cancel the effect of former reconnection of the same string pieces).

- the implementation of the space-time evolution of the showers permitted the study of self-interactions of strings and, hopefully, provided a more realistic simulation as a whole. The effect on the uncertainty on the W mass is more complex: on one side, the average parton density decreases, on the other side, the strings have more time to interact.

Apart from remaining approximations, there is one shortcoming in the model: the colour reconnection is made after the generation of the whole parton shower, and therefore does not influence its development.

4 String reconnection in $Z^0 \to q\bar{q}$ decay

The extension of the idea of reconnection to the inside of a shower appears as a natural step when studying colour reconnection. In some sense, it brings the investigation back to a known area, since an impressive amount of experimental data from hadronic Z^0 decays is available. On the other hand, the problematic of the Monte-Carlo simulation of QCD processes is far from being solved.

The direct comparison of a Monte-Carlo which includes colour reconnection with real data is complicated by the fact that the generators used to describe the data already contain several adjustable parameters which can absorb effects due to colour reconnection though they are not introduced for this purpose. Ideally, tuning should be made on event shapes which are not affected by reconnection. The search for such a set of variables remains to be done.

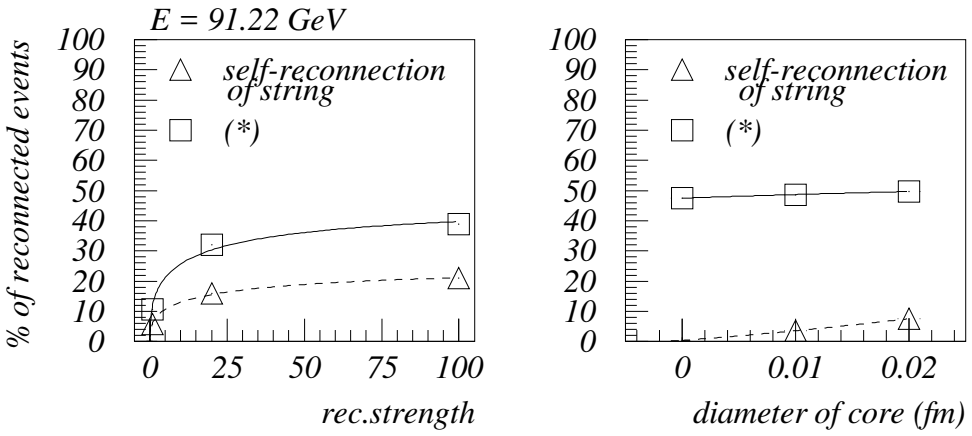

Figure 13: *Relative number of reconnected events as a function of the free parameter R_s (flux tubes) and of the core* diameter *(vortex lines). (*) including reconnection after gluon branching (Fig. 3).*

- reconnection rate

  On Fig. 13 the fraction of events with reconnection is shown . For comparison, the results with reconnection from Fig. 3 (after gluon branching) and without it are presented. This type of glueball production causes about a half of reconnections of flux tubes and an overwhelming majority of vortex line's reconnections (where each gluon branching results in a glueball production).

- final multiplicity

  In Table 1 the mean charged multiplicity in hadronic Z^0 decays is shown for various reconnection model assumptions. The extreme case (vortex lines with non-suppressed glueball production) gives about 7% less charged particles. In case of flux tubes, the decrease in charged multiplicity corresponding to the beginning of the saturation plateau amounts to 4%.

reconnection after gluon branching incl.	no reconnection	flux tubes (R_s=1.)	flux tubes (R_s=20.)	vortex lines (diam.=0.fm)
no	21.31 ± 0.02	21.24 ± 0.04	-	21.30 ± 0.03
yes	-"-	21.08 ± 0.02	20.52 ± 0.03	19.99 ± 0.03

Table 1: Mean multiplicity of final charged particles (hadronic Z^0 decay, E_{cm}=91.22 GeV).

- p_t distributions

  Another effect due to colour reconnection is observed in the p_t^{out}, p_t^{in} distributions (here defined with respect to the Thrust axis) : the distributions are enhanced in the region of high p_t as can be seen in Fig. 14. Presently, the corresponding experimental spectra are not well reproduced by Monte-Carlo simulations (see [4]). The implementation of colour reconnection would improve the agreement with the data (this was already observed in [6], where the ARIADNE Monte-Carlo including colour reconnection [7] was tuned to the DELPHI data).

Colour reconnection also induces a slight increase of the number of reconstructed jets (Fig.15) while jets tend to be more 'narrow', i.e. the rapidity with respect to the jet axis increases (Fig.16).

Generally speaking, inclusive event shapes are not dramatically changed by modest string reconnection. On the other hand, studies of special event topologies [8, 9] may offer the possibility to spot reconnected events. Thus, for the moment, a careful study confronting our predictions with experimental data is awaited.

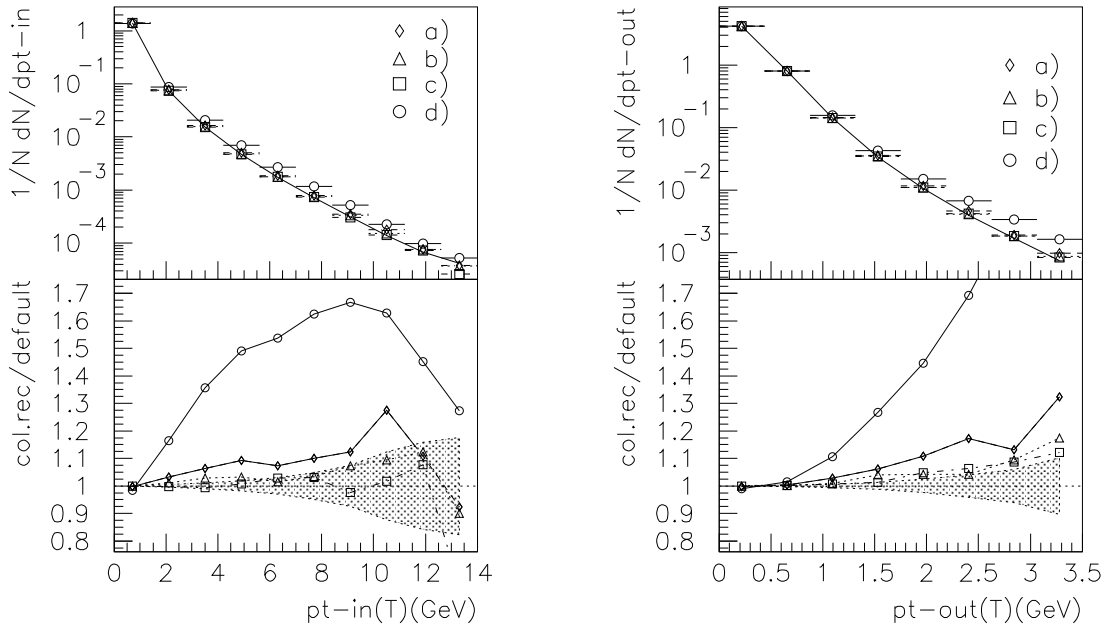

Figure 14: p_t^{in} *and* p_t^{out} *distributions. Comparison of the no-reconnection scheme (full line, JETSET 7.4 PS) with various reconnection scenarii : a)-b) flux tube with rec.strength=1, c)-d) vortex line with core diameter=0. a) and d) include reconnection after gluon branching (Fig. 3).*

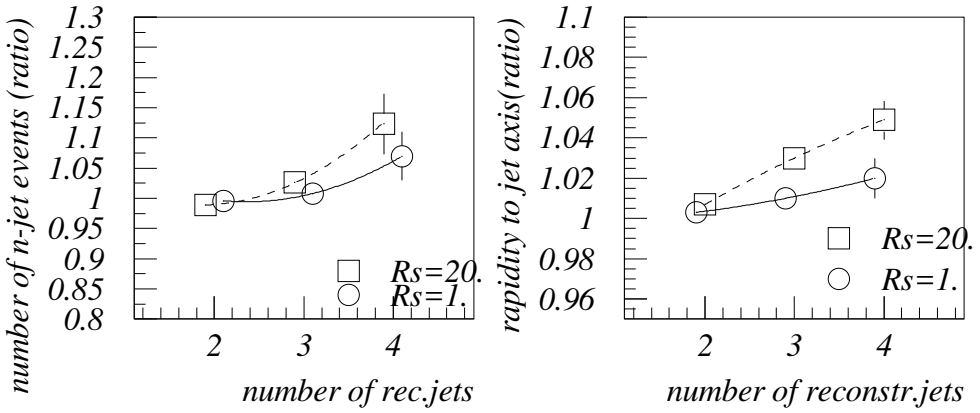

Figure 15: *Ratio of the mean number of 2-,3- and 4-jet events (reconstr. with LUCLUS) obtained with/without reconnection.*

Figure 16: *Mean rapidity of particles belonging to a jet with respect to the jet axis in 2-,3- and 4-jet events. The ratio with/without reconnection is shown (reconstructed with LUCLUS). The flux tube approach is used, with two different values of the reconnection strength R_s.*

5 Colour reconnection in heavy meson decay.

Studies of colour reconnection in high energy processes generally suffer from the lack of direct experimental evidence of the phenomenon. Even if one accepts some observed effects (e.g. p_t behaviour) as an indication of the presence of colour reconnection, the actual reconnection rate cannot be determined. Since this situation is not likely to change soon (unless perhaps a devoted complex study of the LEP1 data sets some limits), one can try to solve the problem with the help of 'colour reconnected' (or 'colour suppressed') decays of heavy mesons. It is not quite obvious that such a parallel between high and low energy processes can be made ; futhermore, the colour suppressed decays of mesons are not fully understood theoretically. Nevertheless, the picture of reconnection as a strong interaction of two colour singlets is valid for meson decays as well as for WW decays.

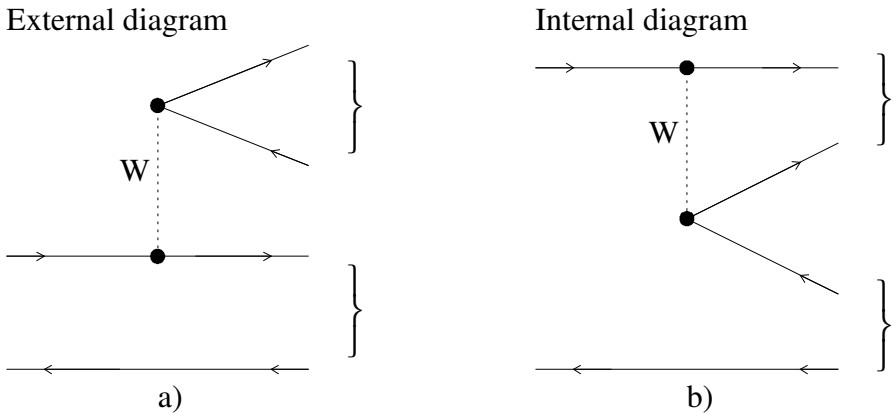

Figure 17: *Spectator Feynman diagrams for meson decay.*

In the following, B^+, D^+ and D_s^+ mesons, which are supposed to decay according to the spectator model (Fig.17), will be studied. The internal diagram can be considered as describing the effect of 'colour reconnection' applied to the external diagram: a strong interaction is needed in order to change the colour configuration of the final state. The external diagram is therefore favoured while the internal diagram is expected to be colour suppressed.

The process can be divided in two steps : 1) heavy quark weak decay , 2) reconnection of colour singlets (strong interaction). The weak part will be described with the matrix element of a free quark decay while a model based on overlaps of colour fields will be used to describe the strong interaction part of the process.

In this approach the meson is viewed as a linear oscillator (pulsating string). The quark and the antiquark moving apart from each other form a string (flux tube) while loosing part of their energy (about 1 GeV/fm). If we consider the string field to be uniform longitudinally (as was

done for W and Z decays) and if quarks are kept on-shell, then the internal dynamics of the meson is fully determined by its mass and by the masses of the constituent quarks.

With these approximations we can apply our model of reconnection to mesons in the same way as we did for string pieces in parton showers. The difference is that now we take into account quark masses and the so-called "yo-yo" effect.

5.1 Experimental branching ratio for colour suppressed decay modes

Our goal is to compare the reconnection probability we get from our model with the branching ratio measured experimentally. Since (at least for the moment) our model does not describe properly the final (reconnected) state (the detailed reconnection mechanism is not included), we will rely on an **inclusive** estimation of the reconnection rate. The measured branching ratio for all reconnected (i.e. colour suppressed) modes will be summed up and compared to the total branching ratio for the decay into final states which correspond to the same quark content (Fig.18):

$$rec.probability = \frac{\Gamma_{internal}}{\Gamma_{external} + \Gamma_{internal}} = \frac{1.}{1. + \frac{\Gamma_{external}}{\Gamma_{internal}}}$$

The full set of branching ratios used is listed in Appendix A. The sums of branching ratios are shown in Table 2 together with their ratio and derived reconnection probability (last column) . The uncertainties have a pure experimental origin. The values obtained suggest that the reconnection is stronger in charm decays than in beauty decays. The same conclusion is drawn from the relative branching ratio for internal/external two body final states with similar masses (see appendix A).

decay mode	$A = \sum(\Gamma_i/\Gamma)_{external}$ [%]	B=$\sum(\Gamma_i/\Gamma)_{internal}$[%]	B/A	B/(A+B)
$B^+ \to u\bar{c}c\bar{s}$	6.2 ± 2.0	0.8 ± 0.2	$0.13^{+0.11}_{-0.06}$	$0.12^{+0.07}_{-0.05}$
$D_s^+ \to s\bar{s}u\bar{d}$	42.5 ± 6	18.0 ± 3.2	$0.42^{+0.15}_{-0.09}$	0.30 ± 0.06
$D^+ \to s\bar{d}s\bar{c}$	8.7 ± 1.9	2.9 ± 1.0	$0.33^{+0.24}_{-0.15}$	0.25 ± 0.11

Table 2: Sum of branching ratios and relative internal/external rate

.

5.2 Reconnection probability from simulated decays

For the simulation of meson decays, a simple generator interfaced with the colour reconnection procedure was written.

Reconnection in decays of heavy mesons was simulated as follows: after the decay of the heavy quark, the daughter quark forms a new meson with a spectator quark and the original

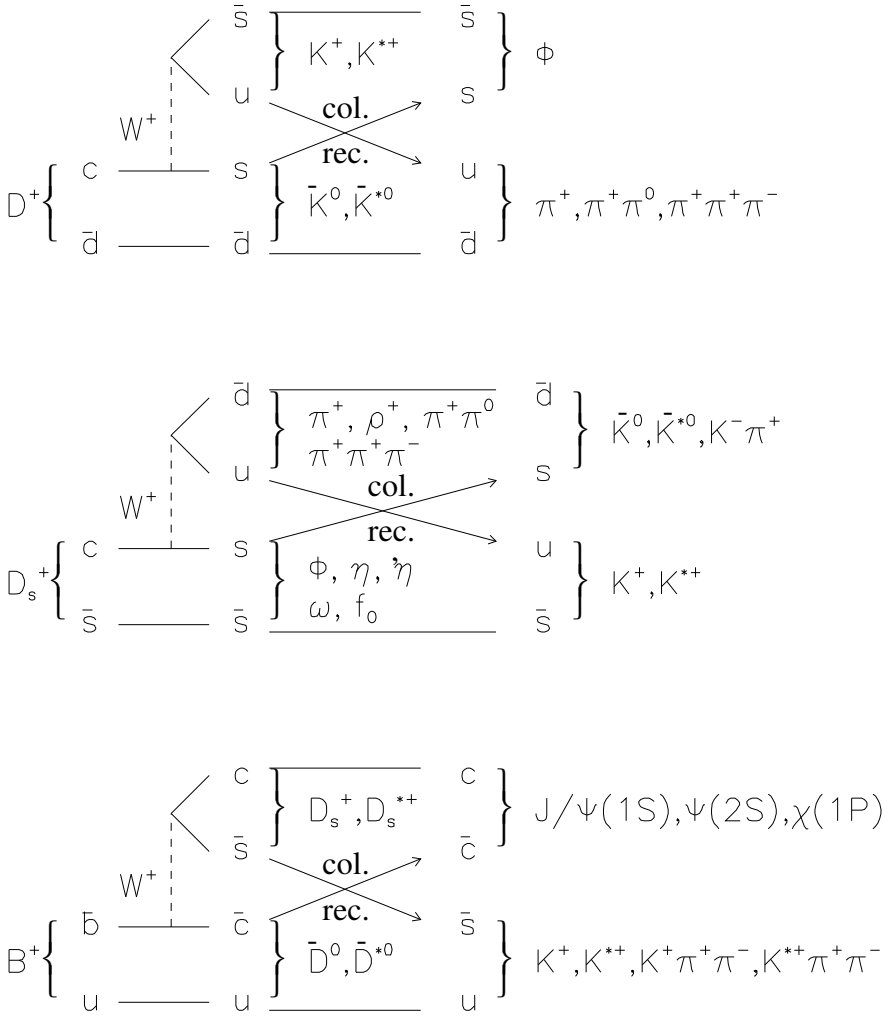

Figure 18: *Quark content of final states in decays under study.*

string piece between them; the mass of this system was required to be equal to the mass of the daughter meson. An additional restriction was implemented in order to keep the orbital momentum of mesons to zero: the original mesons decay always from the "central" position (i.e. the phase of oscillation when quark and antiquark are at the same point and the string between them disappears). If the decay is allowed at any moment, the daughter meson generally gets a non-zero orbital momentum. In addition, the quarks are quasi-free at the "central" point (asymptotic freedom) and the formulae for the weak decay of a free quark may describe the decay well enough.

In hadronic two-body decays the virtual W is required to have the mass of the second meson. Once the W has decayed (its life-time is about 10^{-5} fm/c) the integration of the overlapping colour fields of both mesons (strings) starts (oscillations of strings are taken into account). The integration time is limited to 5 fm/c in the laboratory frame. By this time, the light final states are already well separated and 'heavy' excited resonances have decayed (5 fm/c corresponds to a resonance width of about 40 MeV).

The resulting integral of the overlap is converted in a reconnection probability according to formulae (2). Events are distributed in phase space according to the amplitude of the weak decay (see next section).

It comes out from the study that the reconnection probability depends on the masses of quarks (essentially on the difference between the heavy quark mass and its daughter quark mass) as well as on the masses of the final state mesons (i.e. heavy final state mesons remain 'in touch' much longer and are more likely to be reconnected because they are slow). The dependence of the reconnection probability on the reconnection strength (which is the free parameter of the model) is shown in Fig.19, Fig.20 and Fig.21 for various c and b quark masses (assuming $m_u = 0.005GeV, m_d = 0.01GeV$).

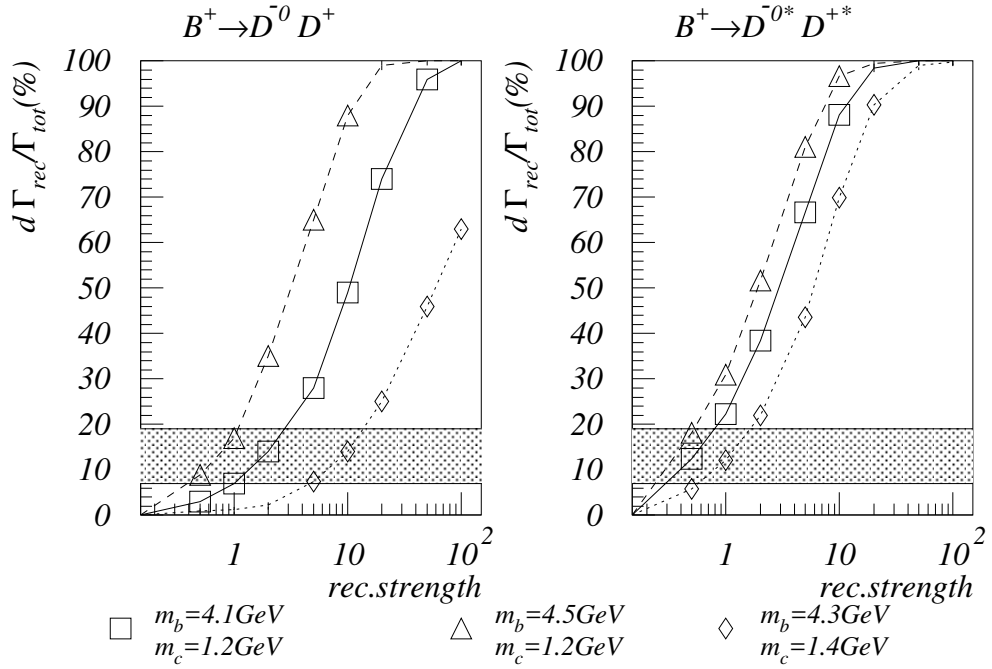

Figure 19: *Reconnection probability in B^+ decays. The shaded area indicates the 'inclusive' reconnection probability derived from the branching ratios measured experimentally.*

Several features can be noticed on the figures: the reconnection probability is higher for

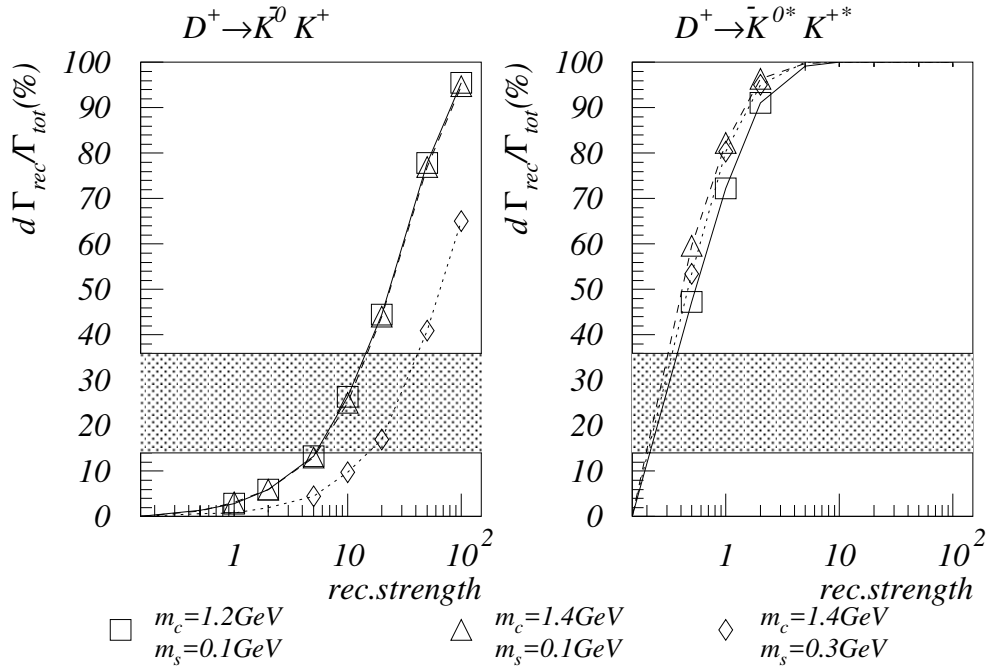

Figure 20: *Reconnection probability in D^+ decays. The shaded area indicates the 'inclusive' reconnection probability derived from the branching ratios measured experimentally.*

decays into heavy final states (particularly in the D_s decay), as already mentioned, a feature easily explained by kinematics.

Furthermore, for decays into heavy final states, the reconnection probability which would correspond to the value measured experimentally (shaded area in Fig.19, Fig.20 and Fig.21) is obtained with a rather small reconnection strength ($\simeq$1.), well bellow the saturation value ($\simeq$20) which came out in the simulation of WW events (see section 2). This suggests that one can set a limit on the amount of reconnection in WW events (see Fig.4).

Fig.19, 20 and 21 also indicate that for heavy final states, the reconnection in D decays is indeed stronger than in B decays (for a given reconnection strength).

It is tempting to conclude that the observed 'reconnected' final states result from reconnection in an intermediate state, most probably formed by heavier, excited mesons. There are however too many uncertainties involved in the model to be conclusive. The reconnection model misses the last part of the process - the formation of the reconnected final states - so that the mass spectrum of the reconnected mesons cannot be checked. There are no 3- or more-body decays in the simulation, nor the possibility of re-reconnection.

So, once again, the result can not be taken for granted. Still, the model, though quite simple, successfully survives the extension to low energy processes and this is of importance for high

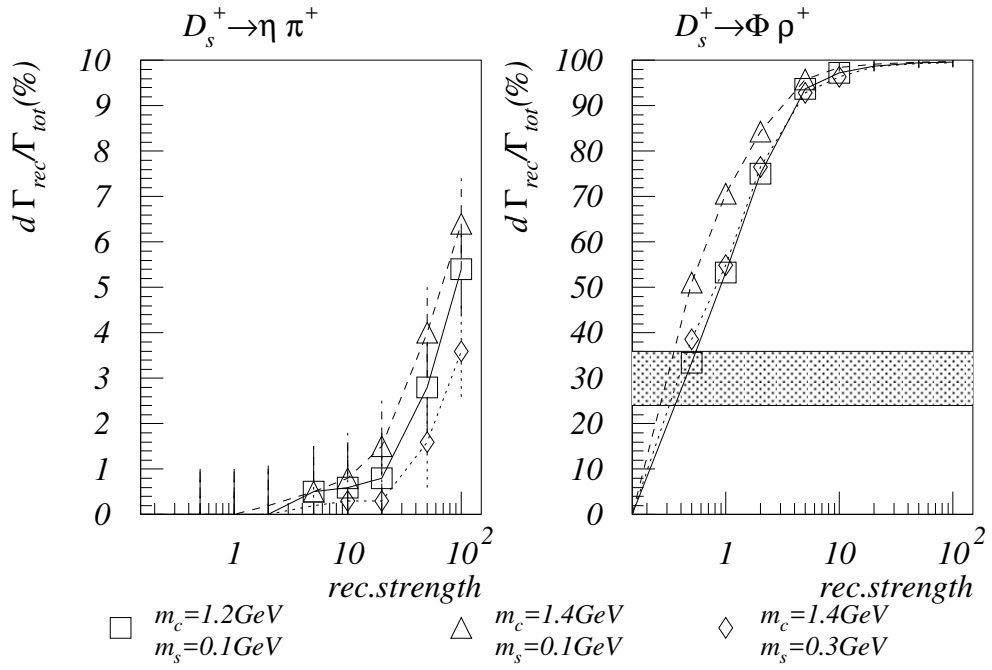

Figure 21: *Reconnection probability in D_s^+ decays. The shaded area indicates the 'inclusive' reconnection probability derived from the branching ratios measured experimentally.*

energy studies.

5.3 Decay rates for exclusive decays ; masses of quarks

As a next exercise, one can check if the matrix element for weak decays gives reasonable decay fractions for various decays of heavy mesons.

Fig.22 a) describes the trajectories of quarks inside the decaying meson. As mentioned in the previous section, heavy quarks are allowed to decay only in the central point when they meet the light quark. There are two arguments leading to this restriction: 1) daughter mesons should not have orbital momentum , 2) very close quarks are quasi-free and should decay according to the formula corresponding to decay of free quarks. Both arguments are not very strong and they are kept mainly because of the simplification they allow in the simulation.(If we allow heavy quarks to decay in an arbitrary phase of oscillation, we will find out that sometimes the formation of daughter mesons is kinematically forbidden. In fact, the region allowed for the formation of light daughter mesons is more or less restricted to the area around the central point).

With the notation derived from Fig.22 b) where a heavy meson with mass M decays in a

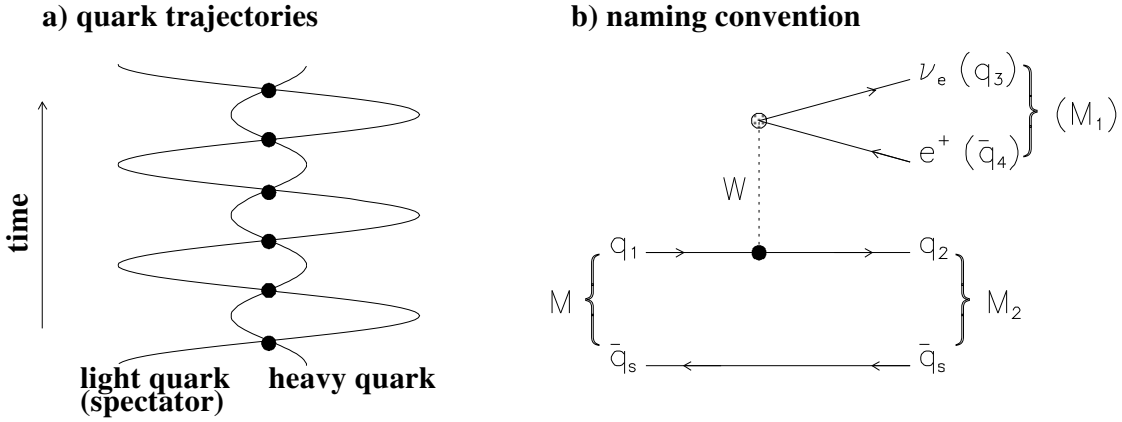

Figure 22: *a) Trajectories of quarks inside a meson. Points mark the so-called "central point" where the heavy quark is allowed to decay. b) Naming convention used in the matrix element.*

meson of mass M_2, the corresponding formula for free quark decays reads as follows:

$$d\Gamma_0 = \frac{(2\pi)^4}{2M} \quad \delta^4(p_1 - p_2 - p_3 - p_4) \quad |M_{if}|^2 d\Phi \tag{9}$$

where $d\Phi$ stands for phase space factor

$$d\Phi = \frac{1}{(2\pi)^9} \quad d^4p_{M_2} \quad d^4p_3 \quad d^4p_4 \quad \delta(p_2^2 - m_2^2) \quad \delta(p_3^2 - m_3^2) \quad \delta(p_4^2 - m_4^2) \tag{10}$$

After reduction of the integration variables by δ functions and after a trivial angular integration we get

$$d\Gamma_0 = \frac{|M_{if}|^2}{(2\pi)^3.8M} \quad \frac{|\vec{p}_{4r}|}{|\vec{p}_s|} \quad \frac{M_2}{E_{M_2}} \; dM_2 \; d\sqrt{q_W^2} \tag{11}$$

where $\vec{p}_{4r}$ is the momentum of the lepton (resp. antiquark $\bar{q}_4$) in the rest frame of the W and $\vec{p}_s$ is the momentum of the spectator quark.

If we now require the daughter quark q_2 and the spectator quark q_s to form a meson with a given mass M_2, we make the convolution with the Breit-Wigner distribution of the invariant mass of the system $(q_2 + q_s)$ (for very narrow resonances the Breit-Wigner distribution becomes in fact a δ function) :

$$d\Gamma_{semileptonic} = d\Gamma_0 . BW(M_2) \overset{\Gamma_{M_2} \to 0}{\longrightarrow} d\Gamma_0 . \delta(\sqrt{(q_2 + q_s)^2} - M_2) \tag{12}$$

In addition, if the W decays in a quark-antiquark pair, there is a similar requirement for the invariant mass of the $(q_3 + q_4)$ system:

$$d\Gamma_{hadronic} = d\Gamma_0 . BW(M_2) . BW(M_1) \overset{\Gamma_{M_2}, \Gamma_{M_1} \to 0}{\longrightarrow} d\Gamma_0 . \delta(\sqrt{(q_2 + q_s)^2} - M_2) . \delta(\sqrt{(q_3 + q_4)^2} - M_1) \tag{13}$$

The matrix element for a heavy quark decay has the form (see naming convention in Fig.22 b))

$$M_{fi} = \frac{-i.G_F}{\sqrt{2}} \sqrt{C} V_{12} V_{34} \bar{u}_2 \gamma_\mu (1 - \gamma_5) u_1 \bar{u}_3 \gamma^\mu (1 - \gamma_5) v_4 \tag{14}$$

where C=1(3) for semileptonic (hadronic) decays.

Neglecting spin-correlations, the corresponding amplitude reads

$$|M_{fi}|^2 = 64CG_F^2|V_{12}|^2|V_{34}|^2 p_1.p_4 p_2.p_3 \tag{15}$$

In principle, spin correlations should be included. However, for heavy quarks the spin becomes independent from momentum and all 4 possible spin final states of meson M_2 (1 for pseudoscalar, 3 for vector meson) should thus have the same production rate. Then, for heavy quarks, we can take

$$|M_{fi}(P \to P)|^2 = \frac{1}{4}|M_{fi}|^2_{non-correlated} \tag{16}$$

$$|M_{fi}(P \to V)|^2 = \frac{3}{4}|M_{fi}|^2_{non-correlated} \tag{17}$$

The recipe seems to work well for semileptonic B decays (Fig.23). (The value of the corresponding element of the Cabibbo-Kobayashi-Maskawa mixing matrix was taken as $V_{cb} = 0.0389 \pm 0.002(stat.) \pm 0.0026(exp.) \pm 0.0017(theor.)$ [10]). The predicted mass of the beauty quark is about 4.3 GeV.

The model however fails for D and D_s decays (dotted lines) since the decay fractions observed experimentally can only be obtained for different masses of the charm quark (1.1 GeV for $D \to \bar{K}^0 e\nu$, 1.4 GeV $D \to \bar{K}^{*0} e\nu$).

It seems therefore necessary to involve the spin structure into the calculations. The helicity amplitudes for semileptonic decays (neglecting lepton masses) are (convention of [11]):

$$|M_{fi}(\lambda_1\lambda_2)|^2 = 32G_F^2|V_{12}|^2(p_1.p_4 p_2.p_3 + \lambda_1\lambda_2 s_1.p_4 s_2.p_3 - \lambda_2 p_1.p_4 s_2.p_3 - \lambda_1 s_1.p_4 p_2.p_3) \tag{18}$$

where $s_i = 2(|\vec{p}_i|, E_i\frac{\vec{p}_i}{|\vec{p}_i|})$; $\lambda_i = \pm 1$ is twice the helicity of the i-th quark.

If we suppose that neither the spectator quark nor the string emit additional gluons there must be a spin flip between q_1 and q_2 if a vector meson is to be produced. In the helicity frame, spin states are defined with respect to the particle momentum. It is therefore necessary to translate spin states from one helicity frame to another:

$$|M_{fi}(P \to P)|^2 = \sum |M_{fi}(\lambda_1 = \lambda_2)|^2 cos^2\frac{\Theta_{12}}{2} + \sum |M_{fi}(\lambda_1 = -\lambda_2)|^2 sin^2\frac{\Theta_{12}}{2} \tag{19}$$

$$|M_{fi}(P \to V)|^2 = \sum |M_{fi}(\lambda_1 = \lambda_2)|^2 sin^2\frac{\Theta_{12}}{2} + \sum |M_{fi}(\lambda_1 = -\lambda_2)|^2 cos^2\frac{\Theta_{12}}{2} \tag{20}$$

where Θ_{12} is the angle between $\vec{p}_1$ and $\vec{p}_2$. P stands for pseudoscalar, V for scalar mesons.

For unpolarized quarks q_1, q_2 we get:

$$|M_{fi}(P \to P)|^2 = 32G_F^2|V_{12}|^2(p_1.p_4 p_2.p_3 + cos\Theta_{12} \cdot s_1.p_4 s_2.p_3) \tag{21}$$

$$|M_{fi}(P \to V)|^2 = 32G_F^2|V_{12}|^2(p_1.p_4 p_2.p_3 - cos\Theta_{12} \cdot s_1.p_4 s_2.p_3) \tag{22}$$

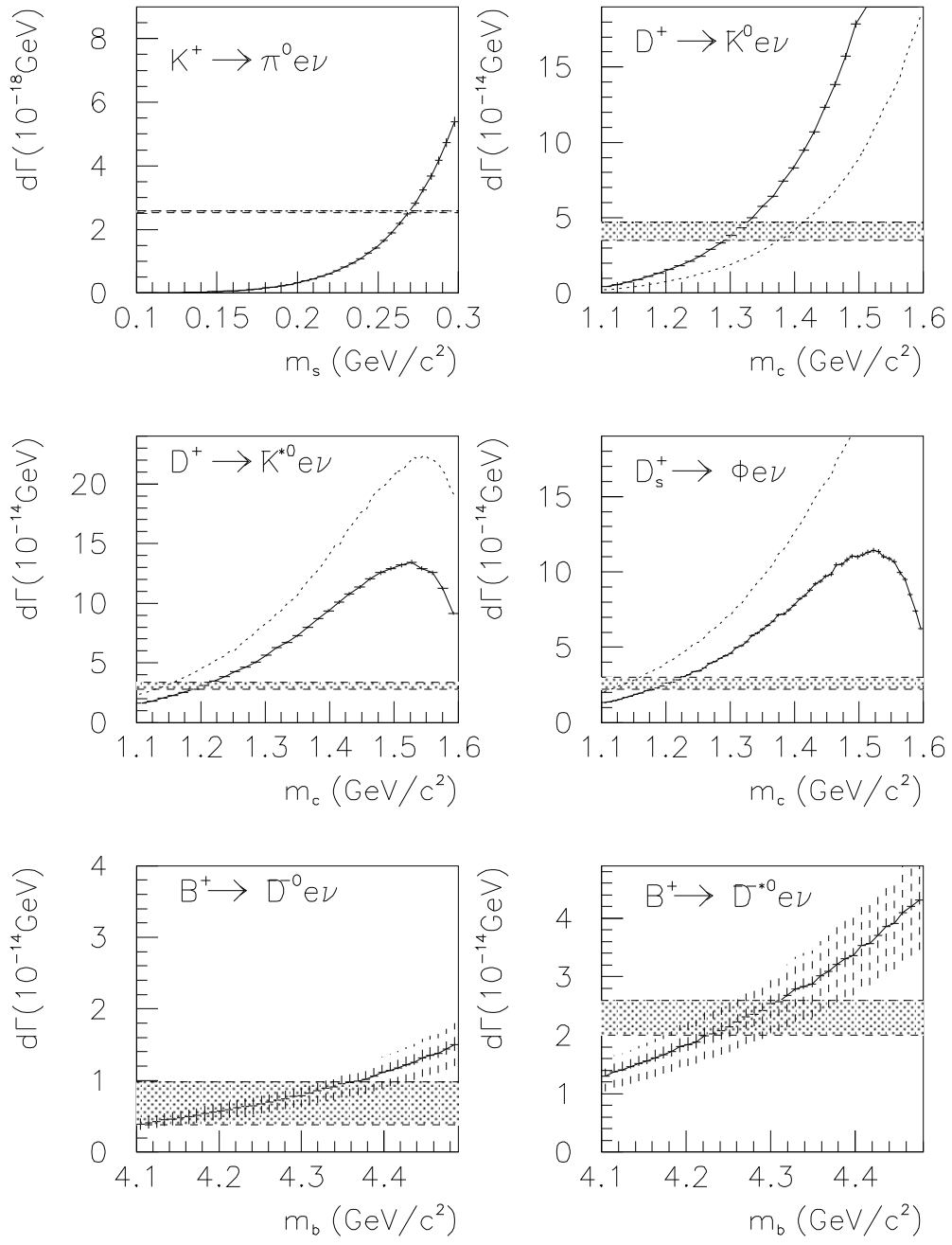

Figure 23: *Partial width of semileptonic decays as a function of heavy quark mass. Horizontal shaded bands indicate the experimental value. See text for a detailed description.*

Using spin related amplitudes improves the results for D meson decays as shown in Fig.23

(full lines), but some discrepancy remains: the decay into pseudoscalar mesons requires the charm quark mass to be around 1.3 GeV, while the decay into vector meson requires it to be around 1.2 GeV.

For semileptonic decays of kaons, the spin correlated amplitude approach gives the measured values if the strange quark mass is $\sim$ 1.27 GeV.

If we now gather the information from all semileptonic decays, our 'best guess' for the effective quark masses is :

$$\begin{aligned} m_u &\sim \quad 0.005 GeV/c^2 \\ m_d &\sim \quad 0.01 GeV/c^2 \\ m_s &\sim \quad 0.27 \pm 0.01 GeV/c^2 \\ m_c &\sim \quad 1.25 \pm 0.05 GeV/c^2 \\ m_b &\sim \quad 4.3 \pm 0.1 GeV/c^2 \end{aligned}$$

These values will be used for the estimation of branching ratios in hadronic decays channels (the expression of each amplitude is given in Appendix B). The comparison of the branching ratio obtained from the generator with the one measured experimentally is made in Table 3.(The reconnection probability for each decay channel is shown as well.) The uncertainties on simulated branching ratios were obtained by varying the quark masses within the limits indicated above. There is a relatively good agreement between the simulated and the experimental decay rates, which seems to corroborate the matrix elements chosen for the weak decay formalism used in this study.

As seen in Table 3, a reconnection strength of about 1 is sufficient to obtain the reconnection rate required by real data. Nothing seems to contradict this value as being also an acceptable scale for our studies at high energies.

Decay mode	Reconnection probability for $R_s = 1.$ [%]	BR from simulation [%]	experimental BR [%]
$B^+ \to \bar{D}^0 D_s^+$	$9.2 \pm 1.$	2.0 ± 0.3	1.7 ± 0.6
$B^+ \to \bar{D}^{*0} D_s^+$	20.2 ± 1.4	1.5 ± 0.3	$1. \pm 0.7$
$B^+ \to \bar{D}^0 D_{*s}^+$	16.7 ± 1.3	1.4 ± 0.3	$1.2 \pm 1.$
$B^+ \to \bar{D}^{*0} D_{*s}^+$	28.4 ± 1.7	1.5 ± 0.3	2.3 ± 1.4
$D^+ \to \bar{K}^0 K^+$	1.7 ± 0.4	0.6 ± 0.2	0.7 ± 0.1
$D^+ \to \bar{K}^{*0} K^+$	8.5 ± 0.9	0.5 ± 0.2	0.4 ± 0.1
$D^+ \to \bar{K}^{*0} K^{*+}$	47.6 ± 2.2	1.8 ± 0.4	2.6 ± 1.1
$D_s^+ \to \eta \pi^+$	$0.$	2.6 ± 0.6	2.0 ± 0.6
$D_s^+ \to \omega \pi^+$	$0.$	1.3 ± 0.4	< 1.7
$D_s^+ \to \eta' \pi^+$	0.6 ± 0.2	1.9 ± 0.5	4.9 ± 1.8
$D_s^+ \to \Phi \pi^+$	0.4 ± 0.2	2.1 ± 0.5	3.6 ± 0.9
$D_s^+ \to \eta \rho^+$	$0.$	$5.1^{+5.4}_{-4.4}$	10.3 ± 3.2
$D_s^+ \to \eta' \rho^+$	29.6 ± 1.7	9.2 ± 2.5	$12. \pm 4.$
$D_s^+ \to \Phi \rho^+$	47.3 ± 2.2	$10.6 \pm 3.$	6.7 ± 2.3

Table 3: Reconnection probability and branching ratios for exclusive hadronic decays.

6 Conclusions

Colour reconnection was studied in the frame of the string model, assuming that the probability of reconnection is correlated with the distance between strings. The consequences of string reconnection were studied by inserting the reconnection procedure between the JETSET parton showering and the fragmentation. Since the real amount of reconnection is unknown, the reconnection strength was varied until a saturation region was reached. This allows at least to predict an upper limit of the expected effects.

String reconnection is found to reduce the final particle multiplicity (by as much as 8 % in extreme cases). This is due to the tendency of reconnection to decrease the invariant mass of strings, making them 'shorter' in momentum space.

An other relevant feature of string reconnection is the enhancement at high values of p_t^{in} and p_t^{out} distributions in hadronic Z^0 decays. Experimental data from LEP1 are not well reproduced by the Monte-Carlo generators in these variables and the agreement is improved by including string reconnection in the simulation. There is of course the problem that little is known about the reconnection mechanism and the expected reconnection rate. The hope is that limits will be found once the reconnection strength is included as a free parameter in the tuning of the generators on real distributions (preliminary results of such tunings indicate that event shape analyses may be able to rule out a reconnection corresponding to the saturation level).

On a very general ground , the observed 'colour suppressed' decays of B mesons into charmonium requires precisely the kind of 'reconnection' (strong interaction changing the colour flow) which we would like to describe in our model. If so, the observed branching ratio can provide a crude 'calibration' of the model. This was done, and the reconnection strength indicated by B^+, D_s^+, D^+ meson decays ($\sim$ 1) is well below the saturation and could allow to reduce the systematic uncertainties related to colour reconnection.

At the generator level, the upper limit of the shift of the W mass (reconstructed from a sample of '4-jet like' events) is about 50 MeV (saturation value). On the basis of the exercise with heavy meson decays I conclude that the shift should be smaller (20-30 MeV at 175 GeV). The sign of the shift is related to the nature of strings: the simulation with strings of type 'flux tube' gives always a positive shift while reconnection of strings of type 'vortex line' can result in negative shift in mean reconstructed W mass.

Acknowledgment

The author is grateful to G.Gustafson, T.Sjöstrand, M.Winter, V.Khoze and J.Polonyi for valuable discussions.

Appendix A

The following experimental branching ratios were considered for the estimation of the reconnection probability [12],[13] :

I) D decay

Decays via external diagrams	*BR* [%]	*Decays via internal diagrams*	*BR* [%]
$K^+\bar{K}^0$	0.7 ± 0.1	$\Phi\pi^+$	0.6 ± 0.1
$K^+\bar{K}^{*0}$	0.4 ± 0.1	$\Phi\pi^+\pi^0$	$2.3 \pm 1.$
$K^{*+}\bar{K}^0$	3.0 ± 1.4		
$K^{*+}\bar{K}^{*0}$	2.6 ± 1.1		
$K^+K^-\pi^+$	0.5 ± 0.1		
$K^+K^-\pi^+\pi_0$	1.5 ± 0.7		
$Sum:$	8.7 ± 1.9	$Sum:$	$2.9 \pm 1.$

II) D_s decay

Decays via external diagrams	*BR* [%]	*Decays via internal diagrams*	*BR* [%]
$\eta\pi^+$	2.0 ± 0.6	$K^+\bar{K}^0$	3.6 ± 1.1
$\eta'\pi^+$	4.9 ± 1.8	$K^+\bar{K}^{*0}$	3.4 ± 0.9
$f_0\pi^+$	1.2 ± 0.5	$K^{*+}\bar{K}^0$	4.3 ± 1.4
$\Phi\pi^+$	3.6 ± 0.9	$K^{*+}\bar{K}^{*0}$	5.8 ± 2.5
$\Phi\pi^+\pi^+\pi^-$	1.8 ± 0.6	$K^+K^-\pi^+$	0.9 ± 0.4
$\eta\rho^+$	10.3 ± 3.2		
$\eta'\rho^+$	$12. \pm 4.$		
$\Phi\rho^+$	6.7 ± 2.3		
$Sum:$	$42.5 \pm 6.$	$Sum:$	18.0 ± 3.2
$Non-classified:$	$K^+K^-\pi^+\pi^0$	$< 9.$	

II) B decay

Decays via external diagrams	*BR* [%]	*Decays via internal diagrams*	*BR* [%]
$\bar{D}^0 D_s^+$	1.7 ± 0.6	$J/\Psi K^+$	0.1 ± 0.01
$\bar{D}^0 D_s^{*+}$	$1.2 \pm 1.$	$J/\Psi K^+\pi^+\pi^-$	0.14 ± 0.06
$\bar{D}^{*0} D_s^+$	$1. \pm 0.7$	$J/\Psi K^{*+}$	0.17 ± 0.05
$\bar{D}^{*0} D_s^{*+}$	2.3 ± 1.4	$\Psi(2S) K^+$	0.07 ± 0.03
		$\Psi(2S) K^{*+}\pi^+\pi^-$	0.19 ± 0.12
		$\chi_{c1}(1P) K^+$	0.1 ± 0.04
$Sum:$	6.2 ± 2.0	$Sum:$	0.8 ± 0.2

Appendix B

Amplitudes for hadronic decays used in section 5.3 (for unpolarized quarks) :

$$|M_{fi}(P \to P_{M_1} P_{M_2})|^2 = A \cdot (p_1.p_4 p_2.p_3 + cos\Theta_{12} \cdot s_1.p_4 s_2.p_3 + cos\Theta_{34} \cdot s_4.p_1 s_3.p_2 + cos\Theta_{12} \cdot cos\Theta_{34} \cdot s_1.s_4 s_2.s_3) \quad (23)$$

$$|M_{fi}(P \to P_{M_1} V_{M_2})|^2 = A \cdot (p_1.p_4 p_2.p_3 - cos\Theta_{12} \cdot s_1.p_4 s_2.p_3 + cos\Theta_{34} \cdot s_4.p_1 s_3.p_2 - cos\Theta_{12} \cdot cos\Theta_{34} \cdot s_1.s_4 s_2.s_3) \quad (24)$$

$$|M_{fi}(P \to V_{M_1} P_{M_2})|^2 = A \cdot (p_1.p_4 p_2.p_3 + cos\Theta_{12} \cdot s_1.p_4 s_2.p_3 - cos\Theta_{34} \cdot s_4.p_1 s_3.p_2 - cos\Theta_{12} \cdot cos\Theta_{34} \cdot s_1.s_4 s_2.s_3) \quad (25)$$

$$|M_{fi}(P \to V_{M_1} V_{M_2})|^2 = A \cdot (p_1.p_4 p_2.p_3 - cos\Theta_{12} \cdot s_1.p_4 s_2.p_3 - cos\Theta_{34} \cdot s_4.p_1 s_3.p_2 + cos\Theta_{12} \cdot cos\Theta_{34} \cdot s_1.s_4 s_2.s_3)$$

$$where A = 3 \cdot 16 \cdot G_F^2 \cdot |V_{12}|^2 \cdot |V_{34}|^2 \quad (26)$$

References

[1] T.Sjöstrand,V.A.Khoze:*On Colour Rearrangement in Hadronic WW Events*, Z.Phys.C62(1994)281-309

[2] B.Andersson,G.Gustafson,G.Ingelman,T.Sjöstrand:*Parton Fragmentation and String Dynamics*
X.Artru:*Classical String Phenomenology. How Strings Work.*
Physics Reports 97,Nos.2&3(1983)31-171

[3] *Physics at LEP200*, CERN Yelow Report, CERN 96-01

[4] K.Hamacher,M.Weierstahl: Wuppertal preprint WU B 95-07, DELPHI Note DELPHI 95-80 PHYS 515

[5] A.Gaidot,J.P.Pansart and N.K.Watson:*Colour reconnection and its effects on measurements of* M_W, OPAL Technical Note TN 320,1995

[6] K.Hamacher,M.Weierstahl: private communication

[7] L.Lönnblad:*Reconnecting Colour Dipoles*, CERN - preprint TH/95-218

[8] G.Gustafson,J.Häkkinen:*Colour Interference and Confinement Effects in W-pair Production*, Lund preprint LU-TP 94-9

[9] C.Friberg,G.Gustafson,J.Häkkinen:*Colour connections in* e^+e_- *annihilation*, Lund preprint LU-TP 96-10

[10] DELPHI: *Determination of* V_{cb} *from the semileptonic decay* $B^0 \to D^{*-}l^+\nu$, CERN preprint PPE/96-11

[11] H.E.Haber:*Spin Formalism and Applications to New Physics Searches*, SCIPP 93/49, NSF-ITP-94-30

[12] Particle Data Group, July 1996

[13] CLEO Collaboration: *Exclusive Hadronic B Decays to Charm and Charmonium Final States*, Cornell preprint CNLS 94-1270, CLEO 94-5